Published in AJSE, Vol: 24, Issue:3
Received on 13th May 2026
Revised on 24th July 2026
Published on 31th July 2026

AIUB JOURNAL OF SCIENCE AND ENGINEERING
ISSN: 1608 - 3679 (print) 2520 - 4890 (Online)
https://doi.org/10.53799/6vfxjj89

Thermal Control and Cooling Enhancement using Prescribed Surface Temperature (PST) and Prescribed Heat Flux (PHF) in Radiative MHD Boundary Layer Flow over a Permeable Shrinking Sheet

Emeziem I. Chukwuemeka[1], Uchenna A. Uka[2 *], Edwin Esekhaigbe[3]

***Abstract*—This study investigates the heat transfer characteristics under the influence of Prescribed Surface Temperature (PST) and Prescribed Heat Flux (PHF) thermal conditions on steady, two-dimensional, magnetohydrodynamic boundary layer flow of an electrically conducting fluid over a permeable shrinking sheet embedded in a porous medium, considering the presence of mass suction, thermal radiation, and heat source/sink. The formulated governing equations are transformed, using similarity transformation, to a system of ordinary differential equations. The equations are linearized via the regular perturbation technique, and the resulting equations are solved analytically. The influence of the various flow parameters on the velocity and temperature profiles under the two heating conditions is shown in the form of graphs, while the trends in quantities of physical significance, such as skin friction and Nusselt number, with some flow parameters, are analyzed via tables. The findings demonstrate that suction stabilizes boundary layer flow across a diminishing sheet and highlight the magnetic field's importance as a flow control parameter. Furthermore, the temperature profiles show that the PHF scenario consistently generates higher temperatures than the PST example, resulting in thicker thermal boundary layers. Also, the suction and Prandtl parameters are the most effective mechanisms for boosting heat transfer. It was also found that radiation and heat sources impede heat transmission.**

***Index Terms*— Heat source/sink, Mass suction, MHD boundary layer, Prescribed Surface Temperature, Prescribed Heat flux, Radiation**.

E. I. Chukwuemeka[1] is with Department of Mathematics and Statistics, Michael Okpara University of Agriculture, Umudike, Abia State, Nigeria (email: indomit2001@yahoo.com)

U. A. Uka[2] is with Basic Sciences Department, School of Science and Technology, Babcock University, Ilishan-Remo, Ogun State, Nigeria. (***corresponding author email**: ukau@babcock.edu.ng).

E. Esekhaigbe[3] is with the Department of Mathematics and Computer Science, University of Africa, Bayelsa State, Nigeria. (email: eskhaigbe.edwin@uat.edu.ng).

The list of symbols is given in Tables 1.

TABLE 1: LIST OF SYMBOLS

Symbol	Quantity	S.I. Units [a]
K	permeability	Dimensionless
M	magnetic field strength	Dimensionless
S_w	Mass transfer parameter	Dimensionless
R	thermal radiation	Dimensionless
H_s	heat source/sink parameter	Dimensionless
Pr	Prandtl number	Dimensionless
σ	Electrical conductivity	s/m

I. INTRODUCTION

The boundary-layer flow over moving surfaces has remained an active and productive research area owing to its wide-ranging applications in engineering and manufacturing processes, including polymer and material processing, cooling of metallic sheets, wire drawing, glass-fibre production, crystal growing, paper production, and numerous others. This work aims to fill the following gap:

a) *Examine the boundary layer behavior of heat transfer in hydro-magnetic flow over a permeable shrinking sheet in the presence of mass suction, thermal radiation, and a uniform heat source/sink under the PST and PHF thermal conditions.*

b) *Using distinct non-dimensional variables for the prescribed surface temperature (PST) and prescribed heat flux (PHF) cases to obtain identical similarity equations for the energy field, thereby establishing a unified analytical framework.*

c) *Highlighting the influence of PST and PHF thermal conditions on the thermal boundary layer which is critical to high-temperature-driven processes where thermal control is of optimal importance.*

II. LITERATURE REVIEW

The earliest systematic investigation of boundary layer flow over a continuous surface moving at constant speed was provided by Sakiadis [1]. Later, it was subsequently extended by Crane [2] to the stretching sheet problem, motivated by polymer extrusion processes, wherein the boundary layer flow of an incompressible viscous fluid driven by a linearly stretching sheet was analyzed. Gupta and Gupta [3] examined heat and mass transfer characteristics for flow over a stretching sheet subjected to suction and injection. Wang [4] extended the analysis to three-dimensional flow due to a stretching sheet. Subsequent important contributions to the study of flow over stretching sheets, encompassing diverse flow situations and geometrical configurations, were made by Uka *et al*. [5], Vajravelu and Nayfeh [6], Kumaran and Ramanaiah [7], Magyari and Keller [8], and Pertha *et al*. [9]. Olajuwon and Ohiamire [10], employing perturbation techniques, examined the effects of variable thermal conductivity and heat source/sink on the hydromagnetic flow of a viscous, incompressible, electrically conducting fluid over a stretching sheet near a stagnation point. Using the Homotopy Analysis Method (HAM), Abd El-Aziz Mohamed and Nabil Tamer [11] investigated the combined influence of Hall current and thermal radiation on hydromagnetic mixed convection flow past an exponentially stretching sheet.

Despite extensive research on stretching sheet flows, boundary layer flow over a shrinking sheet has attracted considerable interest in recent years, driven by its numerous industrial applications in material processing, industrial bulk packaging, soil analysis, and related fields. Flowing over a shrinking sheet is characterized by backward flow directed toward a slot. A defining feature of this configuration is that the generated vorticity is not confined within the boundary layer; consequently, a steady flow over a shrinking sheet is not possible unless a sufficient opposing mechanism, such as suction or a magnetic field, is imposed on the surface. This flow configuration was first identified by Wang [12]. Miklavicic and Wang [13] subsequently established that the existence and uniqueness of solutions for flow over a shrinking sheet in both two-dimensional and axisymmetric cases are contingent upon adequate suction. Further investigations of shrinking sheet flows were reported by Fang [14], Fang and Zhang [15], and Noor *et al*. [16]. Bhattacharyya [17] studied the effect of heat source/sink on MHD flow and heat transfer over a shrinking sheet, reporting that the temperature profile is enhanced by the heat source parameter while the heat sink parameter produces the opposite effect. Bhattacharyya *et al*. [18] obtained an analytical solution for the MHD boundary layer flow of a Casson fluid over a stretching/shrinking sheet with mass suction. Their findings revealed a unique closed-form solution for the stretching case, whereas dual solutions were observed for the shrinking case within a certain range of physical parameters; moreover, a sufficiently strong magnetic field was shown to yield a unique similarity solution for the shrinking sheet, independently of other physical parameters. Jankal and Manoj Kumar [19], employing the Runge-Kutta-Fehlberg numerical scheme, examined the effects of mass suction on MHD boundary layer heat transfer past a shrinking sheet. More recently, Emeziem and Asor [20] provided a mathematical analysis of hydro-magnetic flow and heat transfer over a shrinking sheet under conditions of large suction. Uka *et al*. [21] asserted that partial velocity slip may arise along a stretching surface in fluid flow when the fluid includes dispersed particles, such as those found in emulsions, suspensions, foams, and polymer-based solutions.

Thermal radiation exerts a significant influence on heat transfer whenever the temperature differential between the surface and the ambient fluid is large. In practice, many industrial processes are driven by high-temperature conditions, making the understanding of radiative heat exchange in such settings critically important. Thermal radiation finds widespread application in nuclear and space technology as well as in polymer and metal processing industries. Shit and Halder [22] studied the combined effects of radiation and Hall current on MHD flow, heat, and mass transfer over an inclined permeable stretching sheet with variable viscosity. Babu *et al*. [23] numerically investigated the effects of thermal radiation and heat source/sink on MHD heat and mass transfer over a shrinking sheet with mass suction, demonstrating that radiation enhances the thermal boundary layer. Ishak [24] similarly reported on the effect of radiation on MHD boundary layer flow due to an exponentially stretching sheet, using the Keller-box numerical method.

In most manufacturing processes, the quality of the final product is strongly influenced by the rate of heat transfer at the surface. Equally, in the design of engineering equipment such as electronic devices and heat exchangers, precise control of the heat transfer rate is indispensable for optimal performance. Accordingly, the management and control of heat exchange in engineering processes is of paramount importance. In heat transfer analysis, thermal boundary conditions govern the mode of heat exchange between a surface and the surrounding fluid. Two widely employed thermal conditions in fluid flow and thermal engineering are the Prescribed Surface Temperature (PST) condition, in which the surface temperature is specified, as encountered in electronic devices, heat exchangers, and temperature-controlled manufacturing processes; and the Prescribed Heat Flux (PHF) condition, which specifies the rate of heat energy transferred per unit area of a surface. The PHF condition finds practical application in solar devices, heat exchangers, energy storage systems, and aerospace technology. Hitesh Kumar [25] analytically investigated heat and mass transfer in MHD flow over a stretching sheet under the combined influence of radiation, viscous dissipation, and Joule heating with a power-law variable wall temperature. Mahapatra and Nandy [26] used Runge-Kutta integration, analyzed MHD axisymmetric stagnation-point flow and heat transfer over an asymmetrically shrinking sheet, considering both PST and PHF heating conditions. Fadzilah *et al*. [27] extended the work of Sajid and Hayat [28] by incorporating the PHF condition into the energy equation. Uka *et al*. [29] examined the temperature distribution and boundary layer thickness in a fluidic stream across a stretching sheet with viscous heating effects and thermal non-equilibrium. They used the series technique to produce the analytical solution, and the *Mathematica* program was used to perform the numerical simulation. The outcome demonstrated that an increase in the thermal non-equilibrium number caused the temperature to rise. Greesha *et al*. [30] explored the combined effects of thermal radiation, Hall current, non-uniform heat source/sink, and fluid-particle suspension on the flow and heat transfer of a fully two-phase dusty viscous fluid on a stretching surface embedded in a porous medium, considering both PST and PHF boundary conditions. Their results indicated that the rate of heat transfer was higher in the dusty fluid phase than in the clean fluid and that the PHF boundary condition was better suited for effective cooling of the stretching sheet. Also, Gireesha *et al*. [31] investigated the magnetohydrodynamic boundary layer flow and heat transfer characteristics of a dusty fluid over a flat stretching sheet in the presence of viscous dissipation. Sadighi *et al*. [32] examined the numerical investigation examines the behavior of a quiescent couple stress fluid and the associated heat transfer phenomena on a stretching/shrinking cylinder subjected to specified surface temperature and heat flux boundary conditions. The results indicated that the impact of prescribed heat flux on reducing the local Nusselt number is significantly greater than that of prescribed surface temperature for a given Eckert number. Zeeshan et al. [33] investigate the flow and heat transfer of Jeffery fluid past a linearly stretching sheet with the effect of a magnetic dipole using both Runge–Kutta with shooting technique and series solution based on genetic algorithms (GA) and Nelder-Mead (NM) method. They considered two types of thermal process namely prescribed surface temperature (PST) and prescribed heat flux (PHF). Pavithra and Gireesha [34] explored a numerical analysis on the boundary layer flow and heat transfer of a dusty fluid over an exponentially stretching surface in the presence of viscous dissipation and internal heat generation/absorption for both PEST and PEHF cases. The results showed that suction parameter reduces the velocity and temperature profiles for both PEST and PEHF cases.

From the foregoing review, it is evident that the analysis of hydro-magnetic flow and heat transfer over a shrinking sheet under the simultaneous influence of the PST and PHF thermal boundary conditions has received comparatively little attention, despite the considerable body of literature devoted to various aspects of shrinking sheet flows. A distinguishing feature of the present study is the concurrent treatment of both heating modes for flow over a shrinking surface, thereby filling the comparative analysis gap that has not been adequately reported in the existing literature. Previous investigations have generally examined these thermal conditions in isolation, without providing a direct comparative assessment of their influence on MHD boundary layer flow over a permeable shrinking sheet subjected to suction and heat source/sink. The present study, therefore, aims to examine the boundary layer behavior of heat transfer in hydro-magnetic flow over a permeable shrinking sheet in the presence of mass suction, thermal radiation, and a uniform heat source/sink under the PST and PHF thermal conditions. This work holds scientific merit as a theoretical contribution to boundary layer heat transfer analysis by extending radiative MHD flow models over permeable shrinking sheets with dual PST/PHF thermal boundary conditions, potentially offering insights into thermal control for cooling applications in engineering systems, such as heat exchangers, solar collectors, and its technical novelty and practical impact lies on new analytical/numerical solutions and parameter effects, which are beyond standard similarity transformations. A notable analytical contribution of this work is the use of distinct non-dimensional variables for the PST and PHF cases that nonetheless yield identical similarity equations for the energy field, thereby establishing a unified analytical framework. Beyond its theoretical contributions, the study has direct practical relevance to material processing, thermal management systems, and engineering applications involving contracting or expanding surfaces. These considerations constitute motivation for the present investigation.

III. MATHEMATICAL FORMULATION OF THE MODEL

To formulate the defining equations of flow and energy, we make the following basic assumptions.

- The fluid is Newtonian, electrically conducting, and thermally radiating.
- The flow is steady, two-dimensional, induced by a shrinking sheet and contained in the region $y > 0$.
- The sheet is horizontal, permeable, and shrinking with velocity $U_w = -cx$ and embedded in a porous medium.
- The coordinate axes are aligned such that the $x-$axis is along the sheet, in the direction of flow, and the $y-$axis is perpendicular to it. Fig. 1 depicts the model's schematic.
- A strong magnetic field B_o is applied normally to the x-axis, along with the positive y-axis.
- The temperature of the quiescent, ambient fluid in the field far away from the sheet is T_∞.
- The flow is subjected to mass suction and a uniform heat source/sink.

- The magnetic Reynolds number is assumed to be small, ($R_m \ll 1$), rendering the induced magnetic field negligible, and as such, the applied magnetic field is the dominant field. Consequently, the electromagnetic body force is considered.
- Boundary layer ensues during the flow, and as such, its approximation is considered.

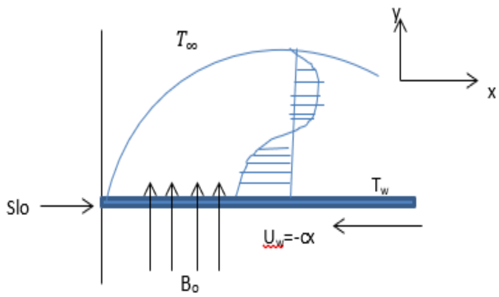

Fig. 1. Schematic diagram of the flow model

Under the assumptions, the governing equations of flow and energy can be expressed as follows.

$\partial u/\partial x + \partial v/\partial y = 0$ (1)

$u\,\partial u/\partial x + v\,\partial v/\partial y = v\,\partial^2 u/\partial y^2 - \sigma B_o^2 u/\rho - vu/k_o$ (2)

$u\,\partial T/\partial x + v\,\partial T/\partial y =$
$k/\rho C_p\,\partial^2 T/\partial y^2 + Q_o(T - T_\infty)/\rho C_p - 1/\rho C_p\,\partial q_r/\partial y$ (3)

Where,
u, v is the x- and y-components respectively, T is the fluid temperature, ρ is the fluid density, v is the kinematic viscosity, k_o is the permeability of the porous medium, σ is the electrical conductivity of the fluid, B_o is the applied magnetic field, T_∞ is the far-field temperature, k is the thermal conductivity of the fluid, C_p is the specific heat capacity at constant pressure, Q_O is the volumetric rate of heat generation or absorption, and q_r is the radiative heat flux.
The corresponding boundary conditions for the velocity components and temperature for the cases of the heating conditions of the model are

Velocity

$$\left.\begin{array}{lll} U = U_w = -cx,\ v = -v_w & & \text{at } y = 0 \\ U \to 0 & \text{as } y \to \infty & \end{array}\right\} \quad (4)$$

Energy
PST Case

$$\left.\begin{array}{ll} T = T_w(x) & \text{at } y = 0 \\ T \to T_\infty & \text{as } y \to \infty \end{array}\right\} \quad (5)$$

PHF case

$$\left.\begin{array}{ll} -k\,\partial T/\partial y = q_w(x) & \text{at } y = 0 \\ T \to T_\infty & \text{as } y \to \infty \end{array}\right\} \quad (6)$$

Where,
U_w is the shrinking velocity, $c > 0$ is the shrinking constant, $v_w > 0$ is the wall mass suction, T_w is the temperature of the sheet. However, the radiative heat flux in (3) can be linearized by employing the Roseland approximation according to Ishak [31-35] such that q_r takes the form

$q_r = -4\sigma^*/3k_+\,\partial T^4/\partial y$ (7)

Where σ^* and k_+ are the Stefan-Boltzmann constant and the mean absorption coefficient, respectively. Assuming that the temperature within the flow is small, T^4 may be expressed as a linear function of temperature using a Taylor series expansion. The Taylor series expansion for T^4 about T_∞, neglecting higher-order terms of $(T - T_\infty)$ gives

$T^4 = 4T_\infty^3 T - 3T^4$ (8)

The equation below is obtained by using (7) and (8) in (3).

$u\,\partial T/\partial x + v\,\partial T/\partial y =$
$k/\rho C_p\,\partial^2 T/\partial y^2 + Q_o(T - T_\infty)/\rho C_p +$
$16\sigma^* T_\infty^3/3\rho C_p k_+\,\partial^2 T/\partial y^2$ (9)

To facilitate the transformation of (1) - (4) into similarity equations, we present the following similarity and dimensionless variables for the two cases of thermal conditions.

PST Case

$$\left.\begin{array}{l} \eta = (c/v)^{1/2} y,\ \psi(x,y) = (cv)^{1/2} x f(\eta), \\ \theta(\eta) = T - T_\infty/T_w - T_\infty,\ T_w - T_\infty = A_o x \end{array}\right\} \quad (10)$$

PHF Case

$$\left.\begin{array}{l} \eta = (c/v)^{1/2} y, \psi(x,y) = (cv)^{1/2} x f(\eta), \\ T = q_w x/k\,(c/v)^{1/2}\theta(\eta) + T_\infty,\ q_w = M_o x \end{array}\right\} \quad (11)$$

Such that ψ is the stream function related to the velocity components in the form

$u = \psi_y$ and $v = -\psi_x$ (12)

Where,
c is a constant of proportionality, η is the similarity variable, $f(\eta)$ and $\theta(\eta)$ are dimensionless velocity and temperature functions, respectively, while A_o and M_o are constants.
The following equations were obtained using (10), (11), and (12) in (1) through (4).

Velocity

$f''' + ff'' - f'^2 - (M^2 + K)f' = 0$ (13)

$$\left.\begin{array}{ll} f = S_w, & f' = -1, \text{ at } \eta = 0 \\ f' \to 0 & \text{as } \eta \to \infty \end{array}\right\} \quad (14)$$

PST Case

$(1 + R)\theta'' + Prf\theta' - Prf'\theta + PrH_s\theta = 0$ (15)

$$\left.\begin{array}{ll} \theta = 1 & \text{at } \eta = 0, \\ \theta \to 0 \quad \text{as } \eta \to 0 & \end{array}\right\} \quad (16)$$

PHF Case

$(1 + R)\theta'' + Prf\theta' - Prf'\theta + PrH_s\theta = 0$ (17)

$$\left.\begin{array}{ll} \theta = -1 & \text{at } \eta = 0 \\ \theta \to 0 & \text{as } \eta \to 0 \end{array}\right\} \quad (18)$$

It's important to note that the prime denotes differentiation and it's with respect to η. Equation (1) is identically satisfied in the transformation. It is observed that the same equation is

obtained for both PST and PHF cases, the difference being the boundary condition at $\eta = 0$ in (16) and (18).
Furthermore, $S_w > 0$ ($V_w > 0$) indicates suction. Additionally, $H_s > 0$ denotes a heat source and $H_s < 0$ denotes heat sink.

IV. METHOD OF SOLUTION

A. Regular Perturbation

The solution approach deployed in this study is the regular perturbation technique. Also known as linearization or asymptotic series expansion method, it's an analytic method for finding the approximate solution of nonlinear equations. This method hinges on the identification of a small parameter, $0 < \varepsilon \ll 1$. The solution is then expressed as a power series in the small parameter, ε. The present methods have proven to be powerful in many areas of applied mathematics, sciences, and engineering. The major criterion for employing the regular perturbation method is the placement of the small parameter, script epsilon,, in the ordinary differential equation (ODE). If the order of the ODE is preserved as $\varepsilon \to 0$. Then the ODE can be solved by applying the regular perturbation method. In other words, if ε appears as a multiplicative factor in a term in the ODE, such that the order of the ODE is preserved and satisfies the boundary condition as $\varepsilon \to 0$. Then, the regular perturbation technique can be employed. Thus, the solution is expressed as a power series expansion in terms of powers of ε, as follows.

$$\sum_{i=0}^{\infty} \varepsilon^i y_i(x) \Rightarrow y(x,\varepsilon) = y_o + \varepsilon y_1 + \varepsilon^2 y_2 + \cdots \qquad (19)$$

The series (17) is substituted into the transformed coupled ordinary differential equations (CODE) and boundary conditions. Then, the coefficients of like powers of ε are selected to obtain a series of equations and solved sequentially. The solutions of $y_i(x)$ are substituted into (19) to obtain an approximate solution of the CODE. The regular perturbation method is a clear and direct approach for obtaining solutions to nonlinear systems without complex convergence criteria and discretization overhead. The procedure adopted in the present work consists of transforming the ordinary differential equations into a similarity equation at large suction, linearizing the resulting nonlinear similarity equations by employing the asymptotic series expansion of the regular perturbation scheme, and solving the resulting linear equations.

B. Similarity Equations at Large Suction

At large suction, $S_w \gg 1$. Thus, according to Bestman [36], we define the following relations to facilitate the derivation of similarity equations.

$$\phi = S_w,\ f(\eta) = S_w F(\phi), \theta(\eta) = \Theta(\phi) \qquad (20)$$

$$F''' + FF'' - F'^2 (M^2 + K)\varepsilon F' = 0 \qquad (21)$$

$$\left.\begin{array}{lll} F(0) = 1, & F'(0) = -\varepsilon & \text{at } \phi = 0 \\ F' \to 0, \text{ as } \phi \to \infty & & \end{array}\right\} \qquad (22)$$

$$(1 + R)\Theta'' + PrF\Theta' - PrF'\Theta + PrH_s\varepsilon\Theta = 0 \qquad (23)$$

PST Case: $\Theta(0) = 1,\ \Theta(\infty) \to 0$ (24)
PHF Case: $\Theta'(0) = -1/S_w,\ \Theta(\infty) \to 0$ (25)
where, $\varepsilon = 1/S_w^2$ (26)

Meanwhile, large values of suction S_w, implies, $\varepsilon \ll 1$ and, as such, serve as the perturbation parameter.

C. Linearization

It is observed from (21) and (23) that the small perturbation parameter, ε multiplies a lower-order derivative. Therefore, it qualifies the equations as a regular perturbation problem. Consequently, we employ the asymptotic series expansion technique of the regular perturbation scheme to linearize the nonlinear similarity equations at large values of S_w. We define a series solution of the form.

$$F(\phi) = 1 + \sum_{n=1}^{\infty} \varepsilon^n F_n(\phi) \qquad (27)$$

$$\Theta(\phi) = \sum_{n=0}^{\infty} \varepsilon^n \Theta_n(\phi) \qquad (28)$$

The following set of ordinary differential equations and their corresponding boundary conditions are obtained using (27), (28) and their derivatives into (21) – (25) and simplifying further.

$O(\varepsilon^o)$: $(1 + R)\Theta_o'' + Pr\Theta_o' = 0$ (29)
$\Theta(0) = 1, \quad \Theta(\infty) \to 0$ (PST) (30)
$\Theta(0) = -1/S_w, \Theta(\infty) \to 0$ (PHF) (31)

$O(\varepsilon)$: $F_1''' + F_1'' = 0$ (32)
$F_1(0) = 0, \quad F_1'(0) = -1, \quad F_1'(\infty) \to \infty$ (31)
$(1 + R)\Theta_1'' + Pr[\Theta_1' + F_1\Theta_1' - F_1'\Theta_o + H_s\Theta_o] = 0$ (33)
$\Theta_1(0) = 1, \quad \Theta_1(\infty) \to 0,$ (PST) (34)
$\Theta_1'(0) = 0, \quad \Theta_1(\infty) \to 0,$ (PHF) (35)

$O(\varepsilon^2)$: $F_2''' + F_2'' + F_1F_1'' - F_1'^2 - (M^2 + K)F_1' = 0$ (36)
$F_2(0) = 0, F_2'(0) = 0, F_2'(\infty) \to 0$ (37)
$(1 + R)\Theta_2'' + Pr[\Theta_2' + F_1\Theta_1' + F_2\Theta_o' - F_1'\Theta_1 - F_2'\Theta_o + H_s\Theta_1] = 0$ (38)
$\Theta_2(0) = 1, \Theta_2(\infty) \to 0,$ (PST) (39)
$\Theta_2'(0) = 0, \quad \Theta_2(\infty) \to 0,$ (PHF) (40)

$O(\varepsilon^3)$: $F_3''' + F_3'' + F_1F_2'' + F_2F_1'' - 2F_1'F_2' - (M^2 + K)F_2' = 0$ (41)
$F_3(0) = 0, F_3'(0) = 0, F_3'(\infty) \to 0$ (42)

V. ANALYTICAL SOLUTION

The solutions of the equations above obtained analytically are as follows.

$F_o = 1$ (43)
$F_1 = -1 + e^{-\phi}$ (44)
$F_2 = -A_1[-1 + e^{-\phi} + \phi e^{-\phi}]$ (45)
$F_3 = 2(A_1)^2[-1 + e^{-\phi} + 1/4\, \phi^2 e^{-\phi} + \phi e^{-\phi}]$ (46)
Where,
$A_1 = 1 - (M^2 + K)$ (47)

PST Case
$\Theta_o = e^{-B_1\phi}$ (48)
$\Theta_1 = -B_3 e^{-B_1\phi} + B_2\phi e^{-B_1\phi} + B_3 e^{-(1+B_1)\phi}$ (49)

$\Theta_2 =$
$- B_6/(1 + B_1)\, e^{-B_1\phi} - B_7(2 + B_1)/(1 + B_1)^2\, e^{-B_1\phi} -$
$B/2(2 + B_1)\, e^{-B_1\phi} - B_4/B_1\, \phi e^{-B_1\phi} + B_5/2B_1\, \phi^2 e^{-B_1\phi} +$
$B_5/B_1\, \phi^2 e^{-B_1\phi} + B_5/B_1^2\, \phi e^{-B_1\phi} + B/(1 + B_1)\, e^{-(1+B_1)\phi} +$
$B_7/(1 + B_1)\, \phi e^{-(1+B_1)\phi} +$
$(2 + B_1)B_7/(1 + B_1)^2\, e^{-(1+B_1)\phi} + B_8/2(2 + B_1)\, e^{-(2+B_1)\phi}$ (50)

Where,
B_1 *to* B_8 are constants and defined as follows.

$$B_1 = Pr/(1 + R)$$
$$B_2 = B_1 + H_s$$
$$B_3 = B_1(B_1 - 1)/(1 + B_1)$$
$$B_4 = (B_1)^2 B_3 + B_1 B_2 - A_1(B_1)^2 + B_1 H_s B_3$$
$$B_5 = B_1 B_2 + B_1 H_s B_2$$
$$B_6 = A_1(B_1)^2 - B_1 B_2 - 2(B_1)^2 B_3 - B_1 H_s B_3$$
$$B_7 = (B_1)^2 B_2 + A_1(B_1)^2 - B_1 B_2 - A_1 B_3$$
$$B_8 = (B_1)^2 B_3$$

PHF Case
$\Theta_o = 1/B_1 S_w\, e^{-B_1\phi}$ (49)
$\Theta_1 = B_2 e^{-B_1\phi} + B_3 \phi e^{-B_1\phi} + B_4 e^{-(1+B_1)\phi}$ (50)
$\Theta_2 = - B_5/B_1^2\, e^{-B_1\phi} + B_6/B_1^3\, e^{-B_1\phi} - B_7/B_1\, e^{-B_1\phi} +$
$B_8/B_1(1 + B_1)\, e^{-B_1\phi} - B_8(2 + B_1)/B_1(1 + B_1)\, e^{-B_1\phi} -$
$\frac{B_9}{2B_1} e^{-B_1\phi} - \frac{B_5}{B_1} \phi e^{-B_1\phi} + \frac{B_6}{2B_1} \phi^2 e^{-B_1\phi} + B_6/B_1^2\, \phi e^{-B_1\phi} +$
$B_7/(1 + B_1)\, e^{-(1+B_1)\phi} + B_8/(1 + B_1)\, \phi e^{-(1+B_1)\phi} +$
$B_8(2 + B_1)/(1 + B_1)^2\, e^{-(1+B_1)\phi} + B_9/2(2 + B_1)\, e^{-(2+B_1)\phi}$ (51)

Where,
B_1 to B_9 are constants and defined as follows.

$$B_1 = Pr/1 + R$$
$$B_2 = H_s + 2B_1 - (B_1)^2/B_1 S_w$$
$$B_3 = B_1 + H_s/B_1 B_w$$
$$B_4 = (B_1 - 1)/B_1 S_w$$
$$B_5 = -(B_1)^2 B_2 + B_1 B_3 - A_1 B_1/S_w - B_1 B_2 H_s$$
$$B_6 = (B_1)^2 B_3 + B_1 B_3 H_s$$
$$B_7 = -B_1 B_4 - (B_1)^2 B_4 + (B_1)^2 B_2 - B_1 B_3 + A_1 B_1/S_w - B_1 B_2 - B_1 B_4 H_s$$
$$B_8 = (B_1)^2 B_3 + A_1 B_1/S_w - B_1 B_3 - A_1/S_w$$
$$B_9 = (B_1)^2 B_4$$

The velocity and temperature profiles are obtained from the equations below.

$f'(\eta) = S_w^2 \sum_{n=0}^{\infty} \varepsilon^n F'_n(\phi)$ (52)
$\theta(\eta) = \sum_{n=0}^{\infty} \varepsilon^n \Theta'_n(\phi)$ (53)

Thus, the analytic solutions for the rate of flow and energy include the following.

Flow Rate
$f'(\eta) = -e^{-\eta} - A_1 \eta e^{-\eta}/(S_w)^2\, A_1 \eta e^{-\eta}/(S_w)^2 -$
$(A_1)^2 \eta e^{-\eta}/(S_w)^4 - (A_1)^2 \eta^2 e^{-\eta}/2(S_w)^4$ (54)

Energy Profile

PST Case
$\theta(\eta) = e^{-B_1\eta} + 1/(S_w)^2 \left[-B_3 e^{-B_1\eta} + B_2 \eta e^{-B_1\eta} +\right.$
$\left. B_3 e^{-(1+B_1)}\eta\right] + 1/(S_w)^4 \left[- B_6/(1 + B_1)\, e^{-B_1\eta} -\right.$
$B_7(2 + B_1)/(1 + B_1)^2\, e^{-B_1\eta} - B_8/2(2 + B_1)\, e^{-B_1\eta} -$
$B_4/B_1\, \eta e^{-B_1\phi} + B_5/2B_1\, \eta^2 e^{-B_1\eta} + B_5/B_1\, \eta^2 e^{-B_1\eta} +$
$B_5/B_1^2\, \eta e^{-B_1\eta} + B_6/(1 + B_1)\, e^{-(1+B_1)\eta} +$
$B_7/(1 + B_1)\, \phi e^{-(1+B_1)\eta} +$
$\left.(2 + B_1)B_7/(1 + B_1)^2\, e^{-(1+B_1)\eta} + B_8/2(2 + B_1)\, e^{-(2+B_1)\eta}\right]$ (55)

PHF Case
$\theta(\eta) = 1/B_1 S_w\, e^{-B_1\eta} + 1/(S_w)^2 \left[B_2 e^{-B_1\eta} + B_3 \eta e^{-B_1\eta} +\right.$
$\left. B_4 e^{-(1+B_1)\eta}\right] + 1/(S_w)^4 \left[- B_5/B_1^2\, e^{-B_1\eta} + B_6/B_1^3\, e^{-B_1\eta} -\right.$
$B_7/B_1\, e^{-B_1\eta} + B_8/B_1(1 + B_1)\, e^{-B_1\eta} -$
$B_8(2 + B_1)/B_1(1 + B_1)\, e^{-B_1\eta} - B_9/2B_1\, e^{-B_1\eta} -$
$B_5/B_1\, \eta e^{-B_1\eta} + B_6/2B_1\, \eta^2 e^{-B_1\eta} + B_6/(B_1)^2\, \eta e^{-B_1\eta} +$
$B_7/(1 + B_1)\, e^{-(1+B_1)\eta} + B_8/(1 + B_1)\, \eta e^{-(1+B_1)\eta} +$
$\left. B_8(2 + B_1)/(1 + B_1)^2\, e^{-(1+B_1)\eta} + B_0/2(2 + B_1)\, e^{-(2+B_1)\eta}\right]$ (56)

D. Skin Friction and Nusselt Number

Two parameters of physical significance are the local skin friction coefficient and the dimensionless coefficient of heat transfer known as the Nusselt number.
The local skin friction, C_{f_x} is given by
$C_{f_x} = 2\tau_w/\rho U_w^2$ (57)
Where,
$\tau_w = \mu\, \partial u/\partial y$, is the wall shear stress.
Hence,
$C_{f_x} = 2R_e^{-1/2} f''(0)$ (58)
Where,
$f''(0) = S_w - A_1/S_w - (A_1)^2/(S_w)^3$ (59)
The Nusselt number is defined as
$Nu = x q_w/k(T_w - T_\infty)$ (60)
Where,
$q_w = -k[\partial T/\partial y]_{y=0}$ is the wall heat flux.
Therefore, for the two cases under consideration, we have
PST Case
$Nu_x = -(1 + R)R_e^{-1/2} \theta'(0)$ (61)
Where,
$\theta'(0) = -S_w B_1 + 1/S_w\, [B_1 B_3 + B_2 - (1 + B_1)B_3] +$
$1/S_w^2\, [B_1 B_6/(1 + B_1) + B_1 B_7(2 + B_1)/(1 + B_1)^2 +$
$B_1 B_8/2(2 + B_1) - B_4/B_1 + B_5/B_1^2 - B_6 + B_7/(1 + B_1) -$
$B_7(2 + B_1)/(1 + B_1) - B_0/2]$ (62)

PHF Case
$Nu_x = (1 + R)/R_e^{-1/2} \theta(0)$ (63)
Where,
$\theta(0) = 1/B_1 S_w + 1/S_w^2\, [B_2 + B_4] + 1/(S_w)^4\, [- B_5/B_1^2 +$
$B_6/B_1^3 - B_7/B_1 + B_8/B_1(1 + B_1) -$
$B_8(2 + B_1)/B_1(1 + B_1) - B_9/2B_1 + B_7/(1 + B_1) +$
$B_8(2 + B_1)/(1 + B_1)^2 + B_9/2(2 + B_1)]$ (64)

From (61) - (63), the dimensionless Nusselt number, Nu_x^+ for the two heating modes takes the form

$$Nu_x^+ = Nu_x/(1+R)R_e^{1/2} = 1/\theta(0), -\theta'(0) \quad (64)$$

VI. RESULTS AND DISCUSSION

The parameter values used to generate each velocity and temperature profile plot are as follows. In figure 2. Impact of magnetic parameter on flow rate. $M = 0.0, 1.0, 1.5, 2.0$ with $S_w = S = 2.0, k = 0.5$.
In figure 3. Impact of suction on flow rate.
$S_w = S = 1.0, 1.5, 2.0, 2.5$ with $M = 2.0,\ k = 0.5$.
In figure 4. Impact of permeability parameter on flow rate. $K = 0.0, 0.5, 1.0, 2.0$, with $M = 1.0,\ M = 3.0, S_w = S = 2.0$.
In figure 5. Impact of magnetic parameter on temperature. $M = 1.0, 3.0, 5.0$, with $S_w = S = 2.0, H_s = 0.5, K = 0.5,$. $R = 1.0, Pr = 0.7$.
In figure 6. Impact of mass suction parameter on temperature. $S_w = S = 2.0, 4.0, 6.0$, with $H_s = 0.5, K = 0.5, R = 1.0$, $Pr = 0.7$.
In figure 7. Impact of heat source/sink on temperature.
$H_s = -0.25, 0.0, 0.25$ with $S_w = S = 2.0, M = 2.0$, $K = 0.5, R = 1.0, Pr = 0.7$.
In figure 8. Impact of Prandtl number on temperature.
$Pr = 0.3, 0.5, 1.0$ with $S_w = S = 2.0,\ M = 2.0, K = 0.5$, $R = 1.0, H_s = 0.5$.
In figure 9. Impact of radiation on temperature.
$R = 0.5, 1.0, 2.0$ with $S_w = S = 2.0,\ M = 2.0, K = 0.5$, $Pr = 0.7, H_s = 0.5$
In figure 10. Impact of permeability on temperature.
$K = 1.0, 3.0, 5.0$ with $S_w = S = 2.0,\ M = 2.0, Pr = 0.7$, $R = 1.0, H_s = 0.5$.
The solutions for this flow model are obtained using the regular perturbation technique. This technique has proven useful in many areas of applied mathematics, offering a more direct approach to solving certain nonlinear systems than most numerical methods that rely on discretization and convergence. Consequently, the numerical results are in good agreement with those in the literature, as shown in Table 2. A plot velocity profiles from the present analytical solution alongside a numerical solution to demonstrate that the perturbation solution converges well within the parameter range explored in the work are given as follows.
The effects of the magnetic parameter M^2, the suction parameter S, and the permeability parameter K on the velocity profiles are shown in Figures 4 – 6, while their influence, including that of the heat source/sink H_s, the radiation parameter R, and the Prandtl number, on the temperature profile under the two thermal conditions of PST and PHF is displayed in Figures 7 – 12. Furthermore, the effects of some physical parameters on skin friction and heat transfer rate are analyzed in Tables 3 and 4.
Figure 4 shows the effect of the magnetic parameter on the velocity profile. A transverse magnetic field imposed on an electrically conducting fluid induces an electric field. The interaction between the applied magnetic field and the induced electric field produces the Lorentz force. A higher magnetic parameter implies a stronger Lorentz force. The Lorentz force acts as a resisting force that confines the vorticity generated by the shrinking sheet within the boundary layer. This enables a steady flow over the shrinking sheet.

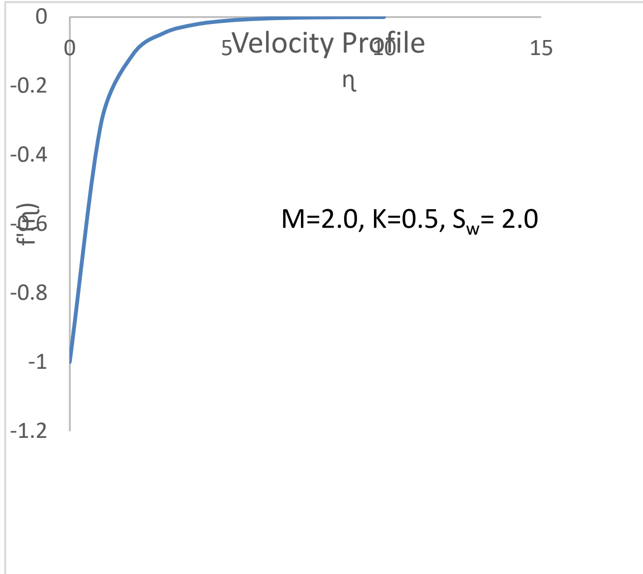

Fig. 2. The plot of analytical solution of velocity profile

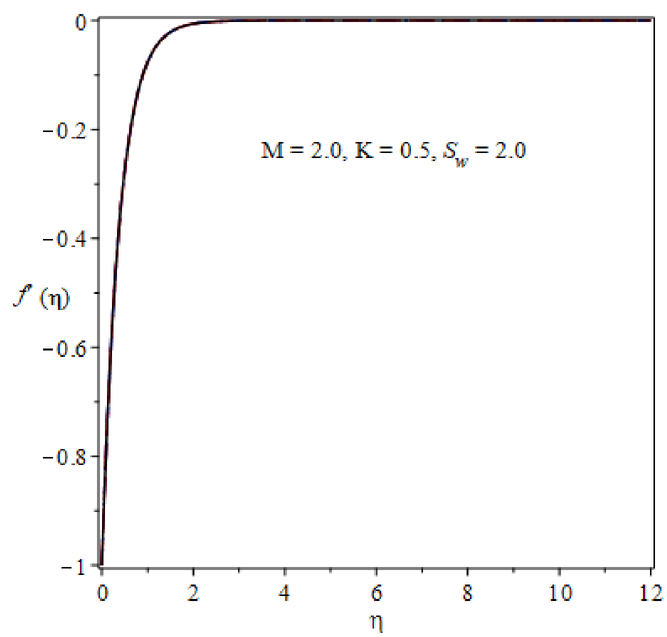

Fig. 3. The plot of numerical solution of velocity profile

Consequently, the boundary layer thickness decreases. Thus, increasing the magnetic parameter enhances fluid velocity. The magnetic parameter is practically important because it controls the flow of the electrically conducting fluid and ensures that heat is transferred at the desired rate. In the manufacturing process, the quality of the final product depends largely on the rate of heat transfer, and the cooling fluid that is meant to cool the shrinking sheet plays an important role in determining the desired property of the product. Therefore, proper regulation of the fluid flow is very important, and this can be achieved through the presence of an external magnetic field. The influence of the mass suction/injection parameter is depicted in Figure 5. It is observed that at low suction, there is a pronounced drop in the fluid velocity away from the wall, which is indicative of boundary layer detachment. As the suction parameter increases, the fluid velocity rises rapidly, moving closer to the sheet and approaching the far-field condition more quickly. This indicates that strong suction is needed to sustain flow over a shrinking sheet. As a result, the thickness of the momentum boundary layer decreases. Physically, this is because, on shrinking surfaces, fluid is drawn toward the surface, and, because of frictional resistance in the form of viscosity, this leads to the accumulation of low-momentum fluid at the wall. Increasing suction removes accumulated fluid, which restrains the instability generated, leading to sustained steady flow over the surface. Thus, suction can be useful in turbulence control and thermal management.

Figure 6 shows the impact of the permeability parameter on the velocity profile, with an interesting behavior noticed in flow dynamics. For values of the magnetic parameter, $M^2 \leq 1$, fluid velocity increases with increasing values of the permeability parameter, but with $M^2 > 1$, the fluid velocity decreases with rising values of the permeability parameter.

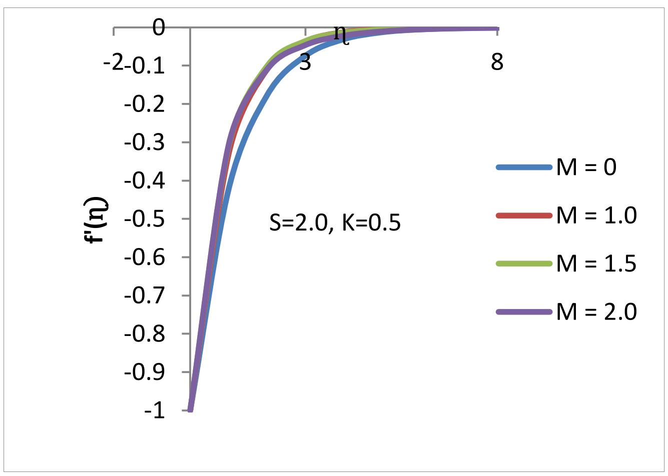

Fig. 4. Impact of magnetic parameter on flow rate

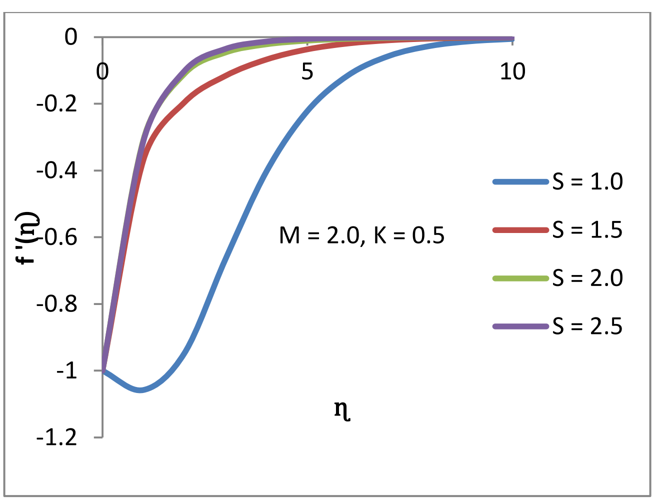

Fig. 5. Impact of suction on the flow rate

This behavior could be attributed to the fact that when the magnetic parameter is small, the permeability parameter becomes a stabilizing force that sustains flow over the sheet. However, with a strong magnetic field $M^2 > 1$, the requirement for the stabilizing influence of the permeability parameter diminishes, and the Lorentz force becomes the dominant stabilizing force that sustains flow.

Figure 7 illustrates the influence of the magnetic parameter on the temperature distribution. As the magnetic field is increased in both the PST and PHF cases, a decreasing trend in temperature is observed, thinning the thermal boundary layer as well as reduction in the thermal boundary layer thickness. Convection at the sheet changes when the magnetic parameter rises, and fluid velocity increases, resulting in a drop in the thermal boundary layer. However, the impact of the PHF case exceeds that of the PST case.

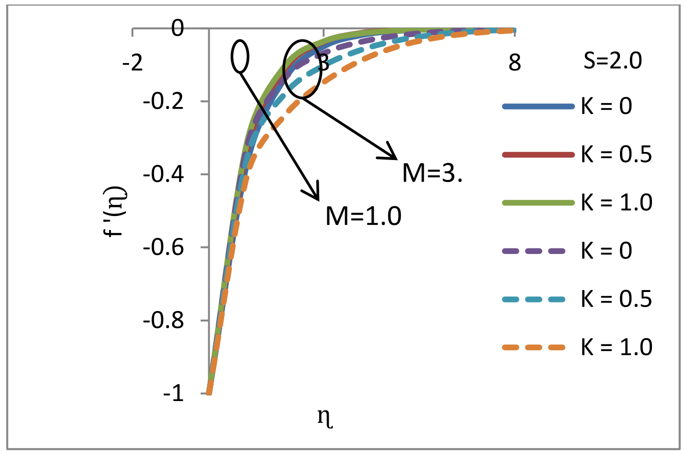

Fig. 6. Impact of permeability on the flow rate

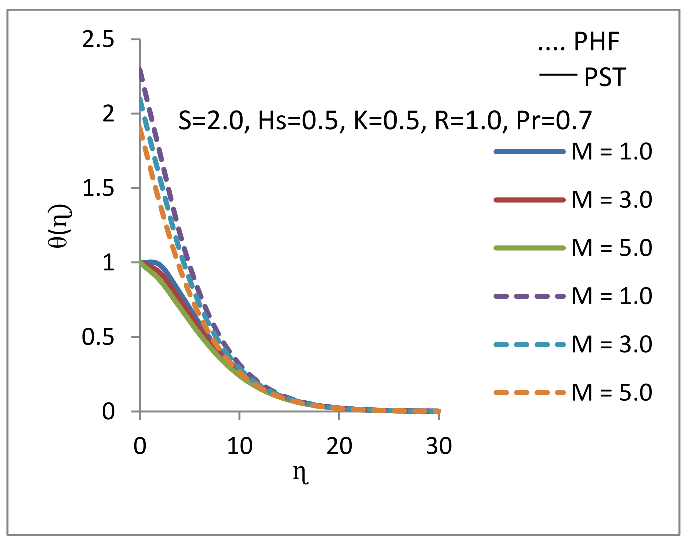

Fig. 7. Impact of magnetic parameter on Temperature

Figure 8 depicts behavior similar to that of the magnetic parameter as the suction parameter increases. As the mass suction parameter increases, both PST and PHF's temperature profiles rapidly decrease. Suction removes low-momentum, heated fluid from the surface, increasing steady flow and decreasing intermolecular interaction, lowering fluid temperature. However, when suction increases, the temperature in the PHF case drops more quickly than in the PST instance. Figure 9 illustrates how the heat source/sink affects the temperature profile. For both PST and PHF, temperature increases with the heat source and decreases with the heat sink. Physically, giving heat raises the temperature, and removing heat decreases it. The PHF case has a higher temperature than the PST case. Figure 10 depicts the influence of the Prandtl number on the temperature profile. The temperature declines fast as the Prandtl number rises under both thermal situations, and the thermal boundary layer thins. A higher Prandtl value indicates poorer heat conductivity and less conduction. Furthermore, the temperature decreases more quickly in the PHF scenario than in the PST case. Figure 11 depicts the effects of radiation on the temperature profile. As the radiation parameter increases, so does the temperature, causing the thermal boundary layer to thicken. An increase in radiation suggests a low mean absorption coefficient in the Roseland approximation, meaning an increase in radiation heat flow. As the radiation parameter increases in the PST case, the surface temperature rises significantly (overshoots). However, the temperature rise is more noticeable in the PHF situation compared to the PST condition. In high-temperature operations, the surface and working fluid produce heat in the form of radiation. Thus, understanding the effect of radiation on flow and heat transfer is critical for designing many sophisticated heat transfer systems that operate at extremely high temperatures. In missile technology, gas turbines, and processes such as polymer and metal processing, where effective thermal control is essential, understanding the impact of radiative heat transfer is critical. Figure 12 depicts a diminishing trend in temperature as the permeability parameter increases for both thermal situations. In keeping with the general tendency, the PHF instance resulted in a thicker thermal boundary layer.

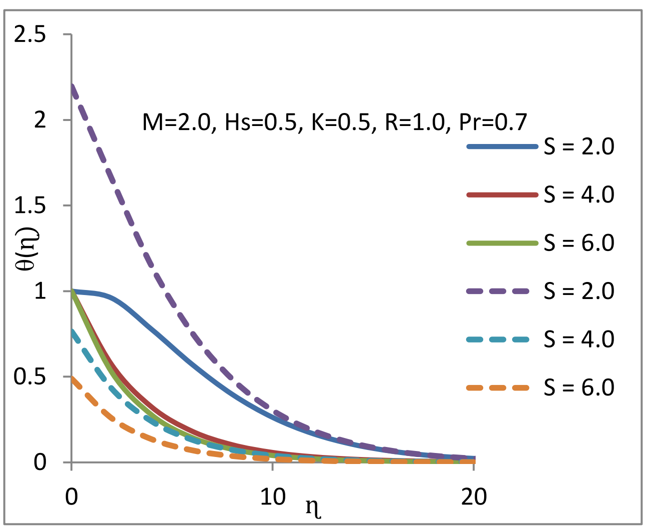

Fig. 8. Impact of mass suction parameter on Temperature

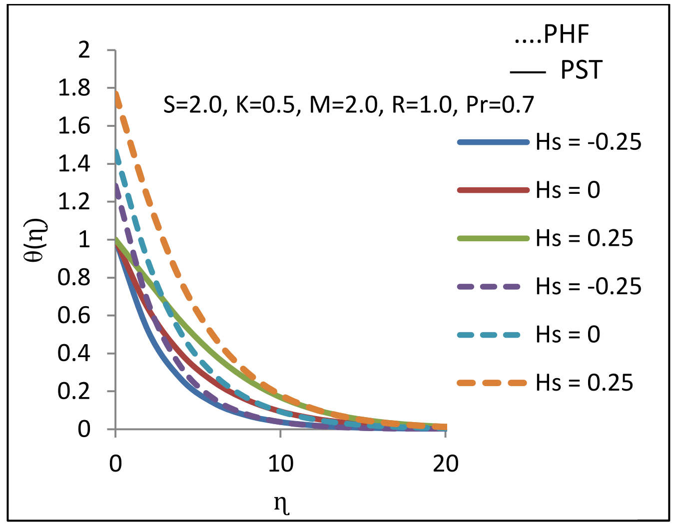

Fig. 9. Impact of heat source/sink on Temperature

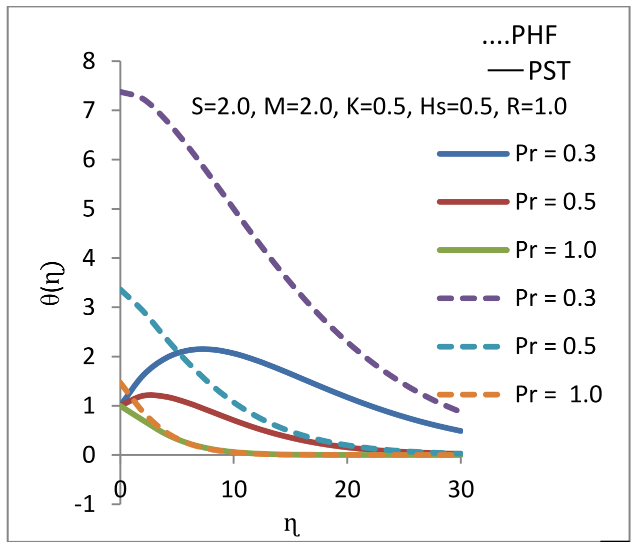

Fig. 10. Impact of Prandtl number on Temperature

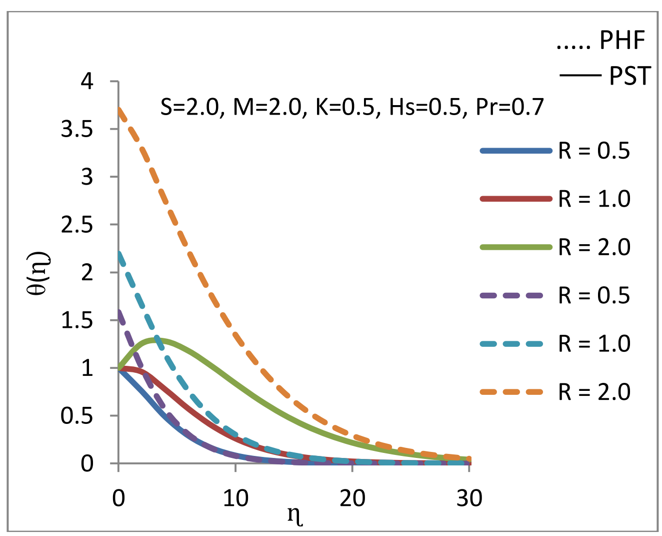

Fig. 11. Impact of radiation on Temperature

Table 2 outlines the influence of some of the physical parameters on the Nusselt number, Nu_x^+ , which expresses the heat transfer rate. From the table, it is observed that Nu_x declines with increasing values of the heat source $(H_s > 0)$ for both the PST and PHF cases. Heat sources introduce additional thermal energy into the boundary layer, thereby reducing the heat transfer rate at the wall, while a heat sink $(H_s < 0)$, displays opposite behavior. With increasing values of Pr, it is noted that the rate of heat transfer enhances significantly for both thermal boundary conditions.

High Pr indicates low thermal conductivity, which reduces heat transmission away from the surface. This causes a narrower thermal boundary layer and a sharper temperature gradient at the surface. As the magnetic field strengthens, Nu_x^+ increases slightly in both the PST and PHF instances. This shows that the magnetic parameter is not the primary convective agent in this flow configuration.

Table 3 shows how suction S_w and radiation R affects Nu_x^+. For both thermal settings, Nu_x^+strengthens significantly as the magnitude of S_w increases. This action demonstrates how suction improves heat transfer at the wall. Physically, suction stabilizes the boundary layer by removing low-momentum and hot fluid from the vicinity of the surface, resulting in a thin thermal boundary layer that enhances heat transfer. However, as the radiation parameter increases, the reverse pattern emerges. Thermal radiation tends to raise the general temperature because the surface emits heat in the form of radiation, which increases the fluid's internal energy and so lessens the temperature gradient at the surface. These patterns are comparable with existing findings in the literature on MHD boundary layer flow over shrinking sheets. The deviations observed in the present results, particularly at the lower suction parameter values ($S_w = 2.0$–2.5), may be qualitatively attributed to the underlying large-suction asymptotic assumption employed in the perturbation formulation. In asymptotic suction boundary-layer theory, the analytical expansion is derived under the assumption that the suction parameter is sufficiently large so that higher-order correction terms become negligibly small and the boundary layer rapidly approaches its asymptotic state. Consequently, when the suction parameter is only moderately large, as in the lower S_w cases of the table, the neglected higher-order terms and nonlinear interactions still contribute appreciably to the thermal field, thereby reducing the accuracy of the asymptotic approximation. This explains why the predicted values of Nu_x^+exhibit stronger deviations at smaller suction levels, whereas the agreement improves progressively as S_w increases from 2.0 to 3.0, where the asymptotic assumptions become more valid and the thermal boundary layer becomes thinner and more stabilized by wall suction. Similar observations regarding the restricted validity of asymptotic suction approximations at moderate or low suction rates have been reported in classical and modern boundary-layer studies, where asymptotic formulations were shown to provide increasingly accurate predictions only in the high-suction regime (Gershbein, 37; Zammert *et al*. 38; Zamir and Young, 39).

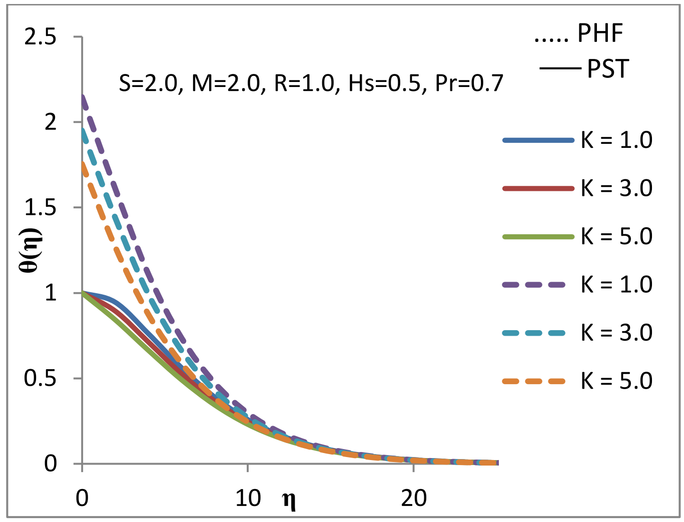

Fig. 12. Impact of permeability on Temperature

TABLE 2: IMPACT OF H_s, Pr AND M^2 ON NUSSELT NUMBER, Nu_x FOR BOTH PST AND PHF CASES

H_s	Pr	M^2	Nu_x^+	Nu_x^+
			PST (Present Study)	PHF (Present Study)
0	0.7	2.0	0.41006	0.68236
0.5	0.7	2.0	−0.13961	0.45532
1.0	0.7	2.0	−0.86784	0.29248
1.0	1.0	2.0	−0.41528	0.48805
1.0	1.5	2.0	0.17971	0.79778
1.0	2.0	2.0	0.71875	1.05785
1.0	0.7	3.0	−0.81983	0.30111
1.0	0.7	4.0	−0.77182	0.31027
1.0	0.7	6.0	−0.67580	0.33035
−1.0	0.7	2.0	0.97367	0.67569
−2.0	0.7	2.0	0.82299	0.28882

TABLE 3: IMPACT OF H_s, S_w, K AND R ON NUSSELT NUMBER, Nu_x FOR BOTH PST AND PHF CASES

S_w	K	R	Nu_x^+	Nu_x^+
			PST (Present Study)	PHF (Present Study)
2.0	0.5	1.0	-0.86784	0.29248
2.5	0.5	1.0	- 0.14640	0.53228
3.0	0.5	1.0	0.30427	0.77569
2.0	1.0	1.0	−0.84384	0.29674
2.0	1.5	1.0	-0.81983	0.30111
2.0	0.5	1.5	-1.15137	0.20303
2.0	0.5	2.0	−1.39733	0.14631

A TERM-BY-TERM ERROR ANALYSIS OVER A RANGE OF s_w VALUES

The thermal response gradually changes as suction increases, and the rate of variation varies considerably between the PST and PHF thermal boundary conditions, according to a term-by-term error analysis of the Nusselt number Nu_x^+ with regard to the suction parameter S_w. The Nusselt number for the PST example at fixed $K = 0.5$ and $R = 1.0$, varies from -0.86784 at $S_w = 2.0$ to -0.14640 at $S_w = 2.5$ and finally to 0.30427 at $S_w = 3.0$. The equivalent subsequent increments are $+0.72144$ and $+0.45067$, respectively, showing that the corrective terms get smaller as suction rises. An approximate relative truncation error of

$$| 0.45067 - 0.72144 |/0.72144 \times 100 \approx 37.53\%.$$

is obtained by reducing the second increment in comparison to the first. This demonstrates that as suction increases, the perturbation contributions gradually converge. Nu_x^+ grows from 0.29248 to 0.53228 and subsequently to 0.77569 for the PHF scenario with the identical assumptions, resulting in increments of 0.23980 and 0.24341. Between these subsequent words, the relative difference is

$$| 0.24341 - 0.23980 |/0.23980 \times 100 \approx 1.51\%.$$

When compared to PST, the extremely small percentage error indicates a very consistent convergence pattern for the PHF solution. As a result, over the investigated suction range, the PHF thermal condition shows improved numerical consistency and smoother asymptotic behavior. The variations in the permeability parameter K also show the solution's convergence properties for constant suction $S_w = 2.0$ and radiation parameter $R = 1.0$. In the PST situation, Nu_x^+ changes from -0.86784 to -0.84384 when K is increased from 0.5 to 1.0, resulting in a correction term of 0.02400. Values of -0.81983, -1.15137, and -1.39733 are produced by further increases to $K = 1.5$ and $K = 2.0$. The further adjustments are -0.33154, -0.24596, and 0.02401. Higher-order terms become more significant at higher permeability values, as indicated by the sudden sign reversal after $K = 1.5$, which suggests slower convergence of the perturbation expansion in the PST configuration. In comparison, the PHF values range from 0.29248 to 0.29674, 0.30111, 0.20303, and 0.14631. The comparable increments are -0.09808, -0.05672, 0.00426, and 0.00437. For small value of K, the solution initially converges smoothly, but higher permeability values introduce stronger nonlinear effects that increase the gap between subsequent terms, even though the solution initially converges smoothly for small value of K. However, the PHF boundary condition offers more numerical stability and less sensitivity to perturbation truncation errors over the studied parameter range, as evidenced by the fact that the amplitude of variation in PHF is still significantly smaller than in PST.

QUANTITATIVE COMPARISON OF THE NUSSELT NUMBER UNDER BOTH CONDITIONS AND EXPLANATION, FROM THE PERSPECTIVE OF THE ENERGY EQUATION AND BOUNDARY CONDITIONS, WHY THE PHF MODE CONSISTENTLY PRODUCES THICKER THERMAL BOUNDARY LAYERS

For almost all parameter combinations, the PHF condition consistently produces higher positive Nusselt numbers than the PST condition for the data shown in Table 2. This indicates weaker wall temperature gradients and, as a result, thicker thermal boundary layers under PHF heating. For example, the PST and PHF Nusselt numbers are 0.41006 and 0.68236 at $H_s = 1.0$, $Pr = 0.7$, and $M^2 = 2.0$, respectively; at $H_s = 1.0$, $Pr = 0.7$, and $M^2 = 2.0$, the values become -0.86784 and 0.29248. The PHF value rises from 0.29248 to 1.05785, while the PST Nusselt number changes from -0.86784 to 0.71875 when the Prandtl number is increased from $Pr = 0.7$ to $Pr = 2.0$ at fixed values of $H_s = 1.0$ and $M^2 = 2.0$. In comparison to the PST example, where the wall temperature is fixed, the constantly higher PHF values show that the imposed constant heat flux permits the wall temperature to dynamically adapt in response to the flow field, therefore minimizing the near-wall temperature disparity. Thermal energy diffuses farther into the fluid before meeting the boundary requirement because, from the perspective of the energy equation, the PHF boundary condition introduces a predefined thermal flux term rather than a prescribed temperature limitation. A thicker thermal boundary layer results from an increase in the thermal diffusion length. The PST condition, on the other hand, immediately fixes the surface temperature, resulting in a steeper temperature gradient close to the wall, a relatively thinner thermal boundary layer, and a higher rate of heat transfer. In both cases the dimensionless energy equation is the same. The difference lies entirely in the thermal boundary conditions imposed at the wall ($\eta = 0$) as shown in Equations (5) and (6).

Despite differences in suction S_w, permeability K, and radiation parameter R, Table 3 shows a similar pattern, with the PHF case continuously generating greater and smoother Nusselt-number distributions than the PST instance. The PST and PHF values are -0.86784 and 0.29248, respectively, at $S_w = 2.0$, $K = 0.5$, and $R = 1.0$; the values increase to 0.30427 and 0.77569 when suction is increased to $S_w = 3.0$. Similarly, the PST Nusselt number changes from -0.86784 to -0.81983 when permeability is increased from $K = 0.5$ to $K = 1.5$ at fixed $S_w = 2.0$ and $R = 1.0$, but the PHF value marginally increases from 0.29248 to 0.30111. The PHF values drop more gradually from 0.20303 to 0.14631 under increased radiation, whereas the PST values drop dramatically from -1.15137 at $R = 1.5$ to -1.39733 at $R = 2.0$. This quantitative behavior shows that the PHF arrangement keeps the thermal field inside the boundary layer more dispersed. Physically, regardless of the local wall temperature, the constant heat-flux boundary condition continuously introduces thermal energy into the fluid, enabling the thermal field to extend farther into the flow zone. As a result, the energy equation creates a thicker thermal boundary layer by balancing conduction and convection across a greater distance from the wall. In contrast, a thinner thermal boundary layer and more abrupt fluctuations in the local heat-transfer rate result from the PST condition's restriction of the wall temperature to a fixed value, which increases the temperature differential close to the surface and limits thermal penetration.

TABLE 4: COMPARISON OF VALUES $f''(0)$ FOR VARIATIONS IN S_w WITH MAKINDE ET AL. [40] AND BABU ET AL [23] WHEN $M^2 = 2, K = 0$

S_w	Makinde *et al*. (MSV)	Makinde *et al.* (DSM)	Babu *et al.* (Numerical)	Present Study
1	-	-	-	1.000000
2	2.4142136	2.414214	2.41448	2.375000
3	3.302776	3.302776	3.30281	3.296296
4	4.2360679	4.236067	4.23607	4.234375
5	-	-	-	5.192000

Table 4 shows a positive skin friction $f''(0)$, which indicates that the fluid exerts a dragging force on the shrinking sheet.

V. CONCLUSION

An analysis of the flow dynamics and heat transfer behavior for the boundary layer magnetohydrodynamic flow over a shrinking sheet embedded in a porous medium with suction, heat source/sink, and thermal radiation effects has been examined under two thermal boundary conditions, namely prescribed surface temperature (PST) and prescribed heat flux (PHF). The results highlight the following points:

- Increase in magnetic field and suction enhances the fluid velocity but diminishes the thermal boundary thickness and reduces the temperature profile.
- Increase in Prandtl number and permeability reduces the temperature distribution, thus leading to a thinner thermal boundary layer, while radiation and heat source produce the opposite effect. With an increase in heat source and radiation, the rate of heat transfer declines in the PST and PHF cases, while a surge in Prandtl and Suction promotes the heat transfer rate.
- An increase in the magnitude of the magnetic field and permeability parameter leads to a marginal increase in the heat transfer rate for both PST and PHF cases.
- The PHF case produced higher thermal boundary layers and had a stronger influence on the various parameters than the PST case.
- Suction and Prandtl parameters are the most effective mechanisms for enhancing the rate of heat transfer, whereas radiation and heat source inhibit heat transfer.
- The PHF boundary condition consistently outperforms PST, making it more suitable for applications requiring efficient thermal management

The results show that suction plays a stabilizing role in sustaining boundary layer flow over a shrinking sheet and highlight the role of the magnetic field as a flow control parameter. Furthermore, it is observed from the temperature profiles that the PHF case consistently produces higher temperature profiles than the PST case, and consequently, thicker thermal boundary layers. As a result, PHF conditions may be more desirable for systems where sustained heating is needed. Consequently, this study fosters a better understanding of MHD flow dynamics and thermal boundary layer behavior for flow over a shrinking sheet. These findings enrich the extant literature and further deepen the understanding of heat transfer behavior, especially when surfaces are exposed to different thermal conditions. It highlights the influence of PST and PHF thermal conditions on the thermal boundary layer. This is critical to high-temperature-driven processes where thermal control is of optimal importance. The thermal boundary layer responds differently to different surface heating conditions. Thermal engineers can leverage the findings to optimize thermal control in industrial processes.

Further studies can consider different geometries or non-Newtonian fluids, a non-uniform magnetic field, and varying fluid properties to further enhance the industrial relevance.

A. *ACKNOWLEDGEMENT*

We are thankful to the reviewers of this paper for their time and contributions.

B. *AUTHOR'S CONTRIBUTION*

E.I. Chukwuemeka conceived and designed the research study. E. I. Chukwuemeka, U. A. Uka, and E. Esekhaigbe contributed to the framing of the study's theoretical structure. E. I. Chukwuemeka obtained the solution to the transformed mathematical equations.

E. I. Chukwuemeka, U. A. Uka, and E. Esekhaigbe contributed to the analysis and interpretation of the results.

E. I. Chukwuemeka, U. A. Uka, and E. Esekhaigbe participated in the review and editing of the manuscript.

The research supervision and administration were carried out by E. I. Chukwuemeka and U. A. Uka.

All authors agree to the submission of the final manuscript for publication.

C. *CONFLICT OF INTEREST*

The authors state that there is no conflict of interest relating to the publication of the manuscript.

D. *AI TOOL USAGE ACKNOWLEDGEMENT*

The authors declare that no artificial intelligence (AI) tools or Large Language Models (LLMs) were utilized during the research, writing data analysis, or editing of the present work.

REFERENCE

1. B. C. Sakiadis, "Boundary Layer Behaviour on Continuous Solid Surfaces: the boundary layer on a flat surface," AIChE Journal, vol. 7, pp. 221-225, 1961.
2. L. J. Crane, "Flow Past a Stretching Plate," *Journal of Applied Mathematics and Physics*, vol. 21, pp. 645-647, 1970.
3. P. S. Gapta, and A. S. Gapta, "Heat and Mass Transfer on a stretching sheet with suction or blowing," *Canadian Journal of Chemical Engineering*, vol. 55, pp. 744-746, 1977.
4. C. Y. Wang, "The three-dimensional flow due to a stretching flat surface," *Physics of fluid*, vol. 27, pp. 1915-1917, 1984.
5. U. A. Uka, E. Edwin, and B. I. Obi, "Analysis of Boundary Layer Thickness and Temperature Distribution in a Fluidic Stream across a Stretching Sheet with

Thermal Nonequilibrium and Viscous Heating Effects," *El Cezeri Journal of Science and Engineering*, vol. 12, no. 2, pp. 134-152, 2025. http://doi.10.31202/ecjse.1513483

6. K. Vajravely, and J. Nayfeh, "Convective heat transfer at a stretching sheet," *Acta Mechanica*, vol. 96, pp. 47-54, 1993.
7. V. Kumaran, and G. Ramanaiah, "A note on the flow over a stretching sheet," *Acta Mechanica*. Vol. 116, pp. 229-233, 1996. Doi: 10.1007/BF01171433.
8. E. Magyari, and B. Keller, "Heat and Mass transfer in the boundary layer on an exponentially stretching continuous surface," *Journal of Physics D: Applied Physics*, vol. 32, pp. 577-585, 1999.
9. M. K. Pertha, P. V. S. N. Murthy, and G. P. Rajasekhar, "Effect of Visions Dissipation on the Mixed Convention Heat Transfer from an Exponentially Stretching Surface," *Heat and Mass Transfer*, vol. 41, pp. 360-366, 2004.
10. B. I. Olajuwon, and J. I. Ohiamire, "Hydromagnetic Flow near a Stagnation Point on a Stretching Sheet with Variable Thermal Conductivity and Heat Source/Sink," *International Journal of Applied Science and Engineering*, vol. 11, no. 3, pp. 331-341, 2013.
11. M. Abd El-Aziz, and T. Nabil, "Homotopy Analysis of Hydromagnetic Mixed Convection Flow past an Exponentially Stretching Sheet with Hall Current," *Mathematical Problems in Engineering*, pp. 1-26, 2012.
12. C. Y. Wang, "Liquid Film on Unsteady Stretching Sheet," *Quarterly of Applied Mathematics*, vol. 48, no. 4, pp. 601-610, 1990.
13. M. Miklavcic, and C. Y. Wang, "Viscous Flow due to a Shrinking Sheet," *Quarterly of Applied Mathematics*, vol. 64, no. 2, pp. 283-290, 2006.
14. T. Fang, "Boundary layer flow over a shrinking sheet with power law velocity," *International Journal of Heat and Mass Transfer*, vol. 51, 5838, 2008.
15. T. Fang, and J. Zang, "Closed-form exact solutions of MHD viscous flow over a shrinking sheet," *Communication on Non-Linear Scientific and Numerical Simulation*, vol. 14: 2853, 2009.
16. N. T. Noor, S. A. Kechil, and I. Hashim, "Simple non-perturbative solution of MHD viscous flow due to a shrinking sheet," *Communication in Non-Linear Scientific and Numerical Solution*, 2009.
17. K. Bhattacharyya, "Effects of Heat Source/Sink on MHD flow and Heat Transfer over a Shrinking Sheet with Mass suction," *Chemical Engineering Research Bulletin*, vol. 15, pp. 12-17. 2011.
18. K. Bhattacharyya, T. Hayat, and A. Alsaedi, "Analytic Solution of MHD Boundary Layer Flow of Carbon Fluid over a Stretching/Shrinking Sheet with Wall Mass Transfer. *Chinese Physical Society*, vol. 22, no. 2, 024702(1-6), 2013. *IOP Publishing Ltd*.
19. A. K. Jankal, and K. Manoj, "MHD Boundary Layer flow past over a shrinking sheet with heat transfer and mass suction," International *Journal of Computational and Applied Mathematics*, vol. 12, no. 2, pp. 441-448, 2017.
20. I. C. Emeziem, and V. E. Asor, "Mathematical Analysis of Hydromagnetic Flow and Heat Transfer Over a Shrinking Sheet for Large Suction," *International Journal of Novel Research and Development*, vol. 8, 2023. d706-d718.
21. U. A. Uka, E. Edwin, A. Musa, and K. Godswill, "Approximate Solution of Viscous Flow Past an Oblate Continuous Nonlinearly Exponentially Stretched Surface," *International Journal of Engineering and Applied Sciences*, vol. 17, no. 4, (1626436), pp. 171-187, 2025. http://dx.doi.org/10.24107/ijeas.1626436
22. G. C. Shit, and R. Haldar, "Thermal radiation and Hall effect on MHD flow, heat and mass transfer over an inclined permeable stretching sheet," *Thermal Science*, vol. 15, no. 2, pp. S195-S204, 2011.
23. P. R. Babu, J.A. Rao, and S. Sheri, "Radiation effect on MHD Heat and Mass Transfer Flow Over a Shrinking Sheet with Mass Suction," *Journal of Applied Fluid Mechanics*, vol. 7, no. 4, pp. 641-650, 2013.
24. N. Ishak, "MHD boundary layer flow due to an exponentially stretching sheet with radiation effect," *Sains Malaysiana*, vol. 40, no. 4, pp. 391-395, 2011.
25. K. Hitesh, "Radiative heat and mass transfer in MHD flow over a stretching sheet under the effect of joule heating and viscous dissipation with variable wall temperature," *Journal of Science and Arts*, vol. 4, no. 55, pp. 1153-1158, 2021.
26. T. R Mahapatra, and S. K. Nandy, "Momentum and Heat Transfer in MHD Axisymmetric Stagnation-Point Flow over a Shrinking Sheet," *Journal of Applied Fluid Mechanics*, vol. 6, no. 1, pp. 121-129, 2013.
27. Md A. Fadzilah, N. Roslinda, and Md A. Noriham, "MHD viscous flow and heat transfer induced by a permeable shrinking sheet with prescribed heat flux," *WSEAS Transactions on Mathematics*, vol. 9, pp. 365-375, 2010.
28. M. Sajid, and T. Hayat, "The application of homotopy analysis method for MHD viscous flow due to a shrinking sheet," *Chaos, Solitons and Fractals*, vol. 39, pp. 1317-1323, 2009.
29. U. Uka, E. Edwin, E. Joseph, and K. Godswill, "Evaluation of Thermal Transfer Efficiency and Nonlinear Shear Effects on Flow Modulation in a Flexible Microfluidic Heat Transfer System," *Sakarya University Journal of Science*, vol. 29, no. 4, pp. 402-425, 2025. https://doi.org/10.16984/saufenbilder.1713546
30. B. J. Gireesha, B. Mahanthesh, S. R. G. Rama, P. T. Manjunatha, "Thermal radiation and Hall effects on boundary-layer flow past a non-isothermal stretching surface embedded in a porous medium with non-uniform heat sources/sinks and a fluid-particle suspension" *Heat Mass Transfer*, 2015. DOI 10. 1007/s00231-015-1606-3.
31. B. J. Gireesha, G. K. Ramesh, and C. S. Bagewadi, "Heat transfer in MHD flow of a dusty fluid over a stretching sheet with viscous dissipation," *Advances in Applied Science Research*, vol. 3, no. 4, pp. 2392-2401, 2012.
32. S. Sadighi, M. Marin, S. Vlase, (2026) "Heat Transfer Analysis of MHD Quiescent Couple-Stress Non-

Newtonian Flow in a Porous Medium over a Stretching/Shrinking Sheet under PST and PHF Conditions: A Numerical Approach," *Journal of Applied Mathematics, Mechanics and Engineering*, vol. 1, no. 1, 2, 2026.

33. A. Zeeshan, and A. Majeed, "Heat transfer analysis of Jeffery fluid flow over a stretching sheet with suction/injection and magnetic dipole effect," *Alexandria Engineering Journal*, Vol. 55, number 3, pp. 2171-2181, 2016, ISSN 1110-0168, https://doi.org/10.1016/j.aej.2016.06.014.
34. G. M. Pavithra and B. J. Gireesha, "Effect of Internal Heat Generation/Absorption on dusty Fluid Flow over an Exponentially Stretching Sheet with viscous Dissipation," *Journal of Mathematics*, Vol. 2013, Article ID 583615, 10 pages http://dx.doi.org/10.1155/2013/583615.
35. N. Ishak, "MHD boundary layer flow due to an exponentially stretching sheet with radiation effect," *Sains Malaysiana*, vol. 40, no. 4, pp. 391-395, 2011.
36. A. R. Bestman, "The boundary-layer flow past a semi-infinite heated plate for two-component plasma," *Astrophysics and Space Science*, vol. 173, pp. 93–100, 1990.
37. É. A. Gershbein, "Asymptotic solution of the three-dimensional multicomponent laminar boundary-layer equations with large suction," *Fluid Dyn*, vol. 10, pp. 570–573, 1975. https://doi.org/10.1007/BF01026698
38. S. Zammert, N. Fischer, and B. Eckhardt, "Transition in the asymptotic suction boundary layer over a heated plate," *Journal of Fluid Mechanics*, vol. 803, pp. 175-199, 2016. doi:10.1017/jfm.2016.514
39. M. Zamir and A. D. Young, "Similar and Asymptotic Solutions of the Incompressible Laminar Boundary Layer Equations with Suction," *Aeronautical Quarterly*, vol. 18, no. 2, pp. 103-120, 1967. doi:10.1017/S0001925900004121
40. O. D. Makinde, V. B. Awati, and N. M. Bujurke, "Dirichlet series and closed-form exact solutions on MHD Casson fluid flow over a permeable stretching/shrinking sheet," *Palestine Journal of Mathematics*, vol. 10, no. 1, pp. 109 -119, 2021.

Dr. Emeziem Innocent Chukwuemeka holds a Bachelor's degree in Mathematics and Computer Science from the Federal University of Technology, Owerri, Nigeria, and a Master's degree in Applied Mathematics from the University of Port Harcourt, Nigeria. He earned his Ph.D. in Applied Mathematics from Michael Okpara University of Agriculture, Umudike, Nigeria, in 2014. His research interests lie in the boundary layer flows of Newtonian and non-Newtonian fluids, magnetohydrodynamics (MHD), heat and mass transfer, and the modelling and analytical solutions of ordinary differential equations arising in fluid mechanics and related physical sciences.

Dr. Uchenna Awucha Uka serves as a Lecturer in the Department of Basic Sciences, School of Science and Technology, at Babcock University. He obtained a B.Sc. (Hons.) in Mathematics from Michael Okpara University of Agriculture, Umudike, in 2017, an M.Sc. in Applied Mathematics from University of Port Harcourt, in 2014, and a Ph.D. in Applied Mathematics from Rivers State University in 2022 (Nigeria). His research interests span fluid mechanics, heat and mass transfer, computational mathematics, and scientific computing applications. His work primarily focuses on ordinary differential equations arising in fluid mechanics and related physical sciences, including mathematical modeling and analytical solution techniques. He utilizes software packages such as Mathematica and Maple to investigate fluid-flow problems that are initially formulated as partial differential equations and subsequently transformed into coupled ordinary differential equations. He has conducted research on boundary-layer flows, magnetohydrodynamic (MHD) flows, Casson and Sisko nanofluids, third-grade and viscoelastic fluids, thermo-diffusion phenomena, Richardson flow, and flow through stretching media. His research projects place significant emphasis on data-driven modeling, tilted fin array configurations, numerical simulations, and high-performance computing techniques for both laminar and complex fluid-flow systems. He is an active member of several professional and academic organizations, including the Mathematical Association of Nigeria (MAN), Nigerian Mathematical Society (NMS), Association of Mathematical Sciences and Optimization (AMSO), International Society of Fuzzy Sets Extensions and Applications (ISFSEA), and International Association of Engineers (IAENG).

Dr. Edwin Esekhaigbe is a senior lecturer at the University of Africa in the Department of Mathematics and Computer Science. He obtained his bachelor of science degree (Mathematics) from Edo State University, Ekpoma (now Ambrose Ali University, Ekpoma) in 1998; master of Science Degree (MSc Applied Mathematics-Mathematical Physics) at the Rivers State university of Science and Technology (now Rivers State University, Port Harcourt) in Applied Mathematics with emphasis in Mathematical Physics in 2008; and Doctor of Philosophy (PhD Applied mathematics) at the Rivers State University, port Harcourt in 2020. His research interest focuses on computational fluid dynamics, heat and mass transfer, MHD, flows in porous media, and rotating flows. He also finds interest in population dynamics and plant interactions. Dr. Edwin Esekhaigbe is a member of the Nigerian Mathematical physics association (NAMP) and the Nigerian Mathematical society (NMS). He has published widely in peer-reviewed journals and presented papers at Conferences. He has published over 25 articles in reputable journals. He has over four years of teaching and research experience.